

Optimization of Ultrasonic Testing System Applicable to High Manganese Steel Rails

Ryuta HIROKAWA¹, Yoshihiro MIZUTANI¹, Yu KUROKAWA², Masumi MAYUZUMI³, Akira TODOROKI¹

**¹Department of Mechanical Sciences and Engineering, Tokyo Institute of Technology;
2-12-1, O-okayama, Meguro, Tokyo, Japan**

**Tel: +81 3 5734 3178, Fax: +81 3 5734 3178; e-mail: rhirokaw@ginza.mes.titech.ac.jp,
ymizutan@mes.titech.ac.jp, atodorok@ginza.mes.titech.ac.jp**

**²Department of Mechanical and Control Engineering, Tokyo Institute of Technology;
2-12-1, O-okayama, Meguro, Tokyo, Japan
e-mail: kurokawa.y.ab@m.titech.ac.jp**

**³Materials for Nuclear Energy Materials Science Research Laboratory, Central
Research Institute of Electric Power Industry; 2-6-1 Nagasaka, Yokosuka, Kanagawa,
Japan
e-mail: mayuzumi@criepi.denken.or.jp**

Abstract

High manganese casting steel rails are currently used at crossing points of railway tracks, due to its high damage tolerance. Since the rail includes large crystal grains and casting defects, general ultrasonic testing (UT) can not be applied to the rail. Thus, new UT method which can be used for the rail is desired. In this study, new ultrasonic imaging method utilizing both the aperture synthesis and signal processing is proposed. Applicability of the proposed method was evaluated by using the high-manganese steel rails with an artificial surface crack. By utilizing proposed method, the ultrasonic image was improved and distributions of large defects can be roughly observed. However, even utilizing our method, small cracks will be hardly detected and planar-crack may be misjudged as point-shaped defects.

Keywords: High Manganese Steel Rail, Ultrasonic Scattering, Aperture synthesis, Time-Frequency Analysis, Ultrasonic Imaging

1.Introduction

High manganese casting steel rails are currently used at crossing points of railway tracks in Japan. These rails contain no less than 11 to 14% of manganese; while, common steel rails contain only about 1%. One of the advantages of using high manganese steel rails is that they have high damage tolerance to fatigue cracks and so a longer life span. General hot-rolled steel rails are regularly inspected by ultrasonic testing (UT). The UT, however, can not be applied to high manganese steel rails since a large number of ultrasonic scattering occurs at their large crystal grains and casting defects in all over the rails. Figure 1 shows example of the ultrasonic signal detected by pulse-echo method on high manganese steel rails with an artificial flaw. A large number of scattered waves are monitored together with flaw echo and back-wall echo^[1]. Thus, it is difficult to apply UT for inspecting fatigue cracks in the rails. As an alternative to UT, visual or penetrant testing (VT or PT) is carried out, though this requires rails to be removed from their anchor points and turned over manually. This series of processes takes the time and money. Thus, this study aims to develop ultrasonic testing method which can detect fatigue cracks as well as large casting defects which have a potential to be an origin of fatigue crack in high manganese steel rails.

In order to make UT applicable to cast steels, several researchers had tried to improve SN ratio of UT signals by following method;

1. Increasing ultrasonic energy — Large transducer^[2], Burst wave as an incident

- signal
2. Using low frequency ultrasonic ——— Low frequency transducer (500kHz, 1MHz)^[2]
 3. Focusing ultrasonic beam ——— Aperture synthesis, Spherical surface transducer^[2]
 4. Using broad band and supersensitive transducer ——— Composite transducer^[3]
 5. Applying signal processing ——— Split spectrum processing^[4], Image processing on 3-D^[5] etc.

While several trials were conducted as mentioned above, only few methods could improve SN ratio of ultrasonic waves in cast steels, especially those with large content of manganese.

In this study, we proposed a new hybrid method combining an ultrasonic-beam focusing method by aperture synthesis and a signal processing technique by wavelet transform. Applicability of the proposed method was evaluated by applying the method to the high-manganese steel rails used for local lines.

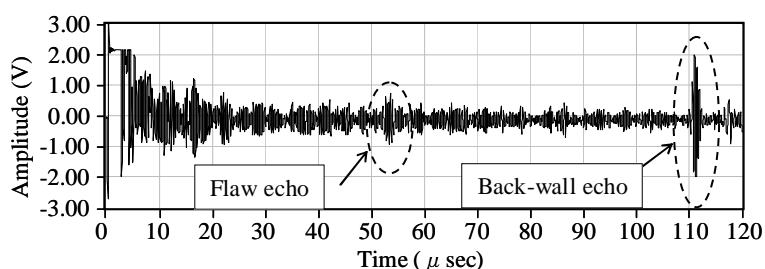


Fig.1 The ultrasonic signal detected by pulse-echo method on a high manganese steel rail with an artificial flaw.

2. Theory

2.1 Outline of the proposed method

The proposed hybrid method is based on an aperture synthesis technique. The procedure of a conventional aperture synthesis method is shown in the left of Fig.2. Ultrasonic signals received at each position on an inspected object are directly used for constructing an ultrasonic image. The concrete procedure of the constructing is explained later.

The right of Fig.2 shows the procedure of the proposed method. Since characteristics of ultrasonic are influenced by frequency, a suitable frequency component for the flaw inspection is selected and extracted by wavelet transform. An ultrasonic image is constructed by aperture synthesis using the extracted frequency components.

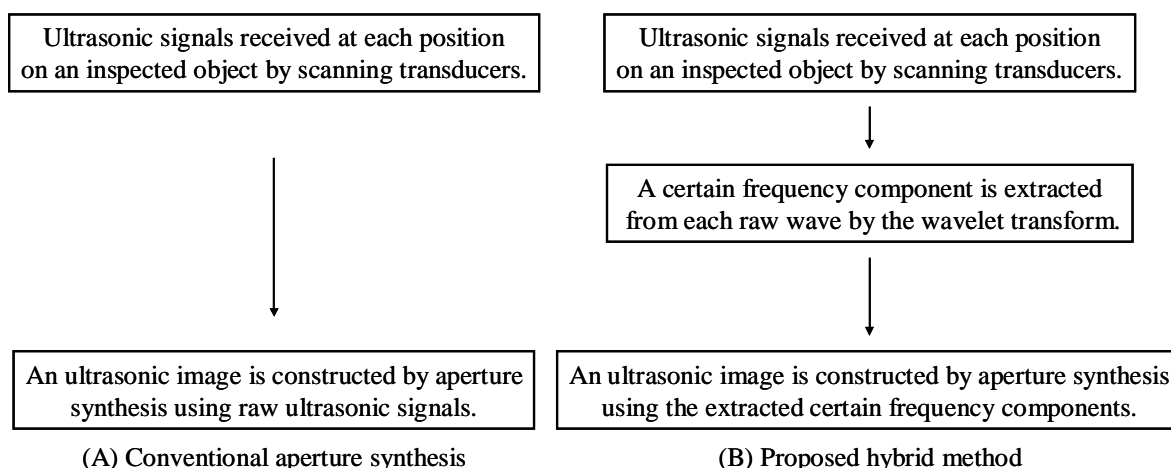


Fig.2 Comparison of conventional aperture synthesis method and proposed hybrid method.

2.2 Wavelet Transform

For extracting a certain frequency component, the continuous wavelet transform is used as a frequency filter. The general wavelet transform of real function $f(t)$ is defined as

$$W(a,b) = \frac{1}{\sqrt{a}} \int_{-\infty}^{\infty} f(t) \psi^* \left(\frac{t-b}{a} \right) dt \quad (1)$$

where $a > 0$ and the superscript * denotes a complex conjugation. The analysis function for the wavelet transform can be defined as equation (2).

$$\psi_{a,b}(t) = \frac{1}{\sqrt{a}} \psi \left(\frac{t-b}{a} \right) \quad (2)$$

Its elements are generated by shifting and scaling a mother wavelet $\psi(t)$. The parameters a and b stand for the scale and shift of the mother wavelet. In this study, the Gabor function was chosen as the mother wavelet. The Gabor function is described as follows.

$$\psi(t) = \frac{1}{\sqrt[4]{\pi}} \sqrt{\frac{\omega_0}{\gamma}} \exp \left[-\frac{1}{2} \left(\frac{\omega_0 t}{\gamma} \right)^2 + i \omega_0 t \right] \quad (3)$$

Fehler! Es ist nicht möglich, durch die Bearbeitung von Feldfunktionen Objekte zu erstellen.

where ω_0 is the center frequency.

2.3 Data Processing

1. Ultrasonic image construction

The conventional ultrasonic image construction method is shown in Fig.3. The intensity at an arbitrary point of an ultrasonic image was determined by taking the sum of ultrasonic amplitude at $2L_i/V$ for each sensor. Here, L_i is the distance between the transducer i ($i = 1 \sim N$) to an arbitrary point. On the other hand, ultrasonic beams have the characteristics of high directivity. Though, an arbitrary points which were out of ultrasonic beam spread angle of the transducer $N = i$ are not affected by ultrasonic beam transmitted from the transducer $N = i$. The ultrasonic signals detected by these transducers were ignored (did not take into account) in the summation process. Ultrasonic beam spread angle φ_0 can be calculated by following equation.

$$\text{Angle of beam spread} = 70 \frac{\lambda}{D_E} \text{ (deg)} \quad (4)$$

here λ is the wavelength in the specimen and D_E is the diameter of the transducer.

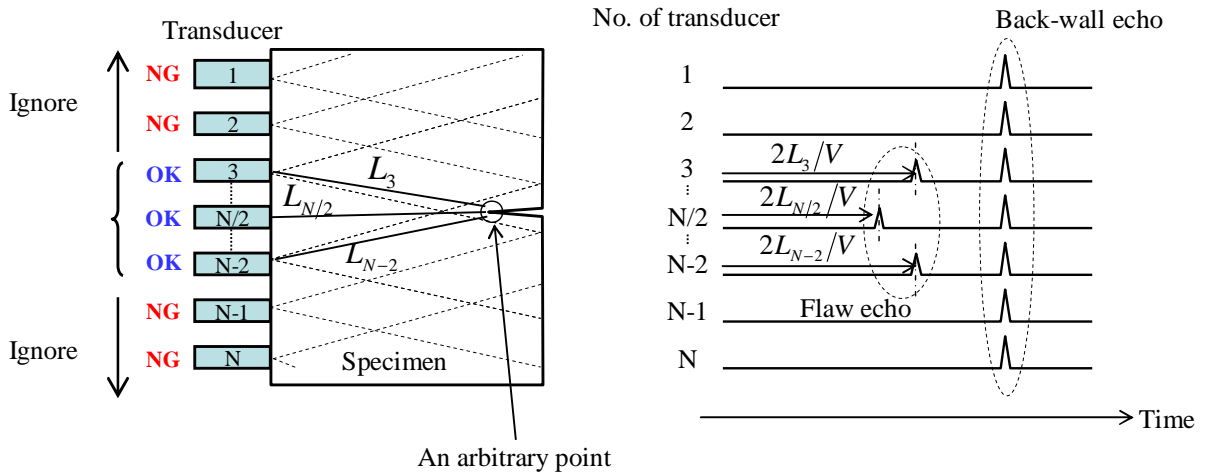


Fig.3 Explanation of a conventional aperture synthesis method.

2. The proposed hybrid method utilizing wavelet transform

Figure 4 shows the detailed explanation of the proposed method. First of all, the real- and imaginary- parts of wavelet coefficients for the ultrasonic signals detected at each position are calculated by equation (1). Then the aperture synthesis is conducted for the real- and

imaginary- data respectively. Finally, the ultrasonic image is constructed by calculating absolute value of complex data at the arbitrary point.

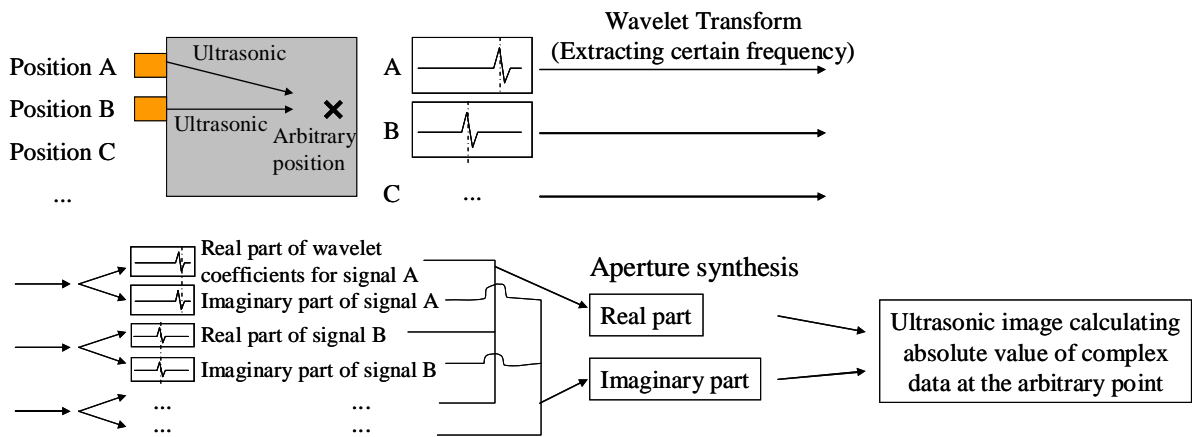


Fig.4 Explanation of the proposed hybrid aperture synthesis method.

3. Experimental Setup

3.1 Specimen

A high manganese casting steel rail (JIS (Japanese Industrial Standard) G5131 SCMnH3) specimen was prepared for the study (see Fig.5). The coordinate system is defined as Fig.5. The y-z plane at x=0 is well polished. It is said that the minimum crack height which should be detected in the field is 5.0mm. In this study, an artificial semielliptical surface crack of 19.8mm length and 6.5mm depth was introduced to the rail using a diamond blade disk (ϕ 20.1mm) on the bottom surface at the center (see Fig.5). The width of introduced crack was 1.0mm.

Figure 6 shows radiographic images of the specimen^[1]. A large number of small casting defects and several large casting defects are existed in the specimen. It is desired that large casting defects and fatigue cracks are detected distinctly by UT.

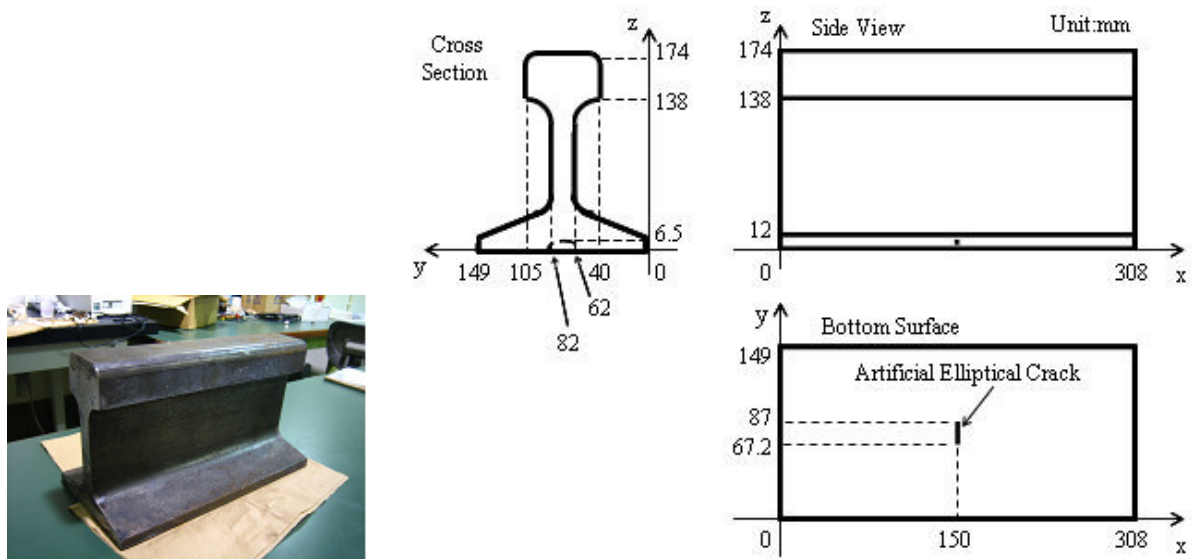


Fig.5 Photograph of the specimen (left) and size of the specimen (right).

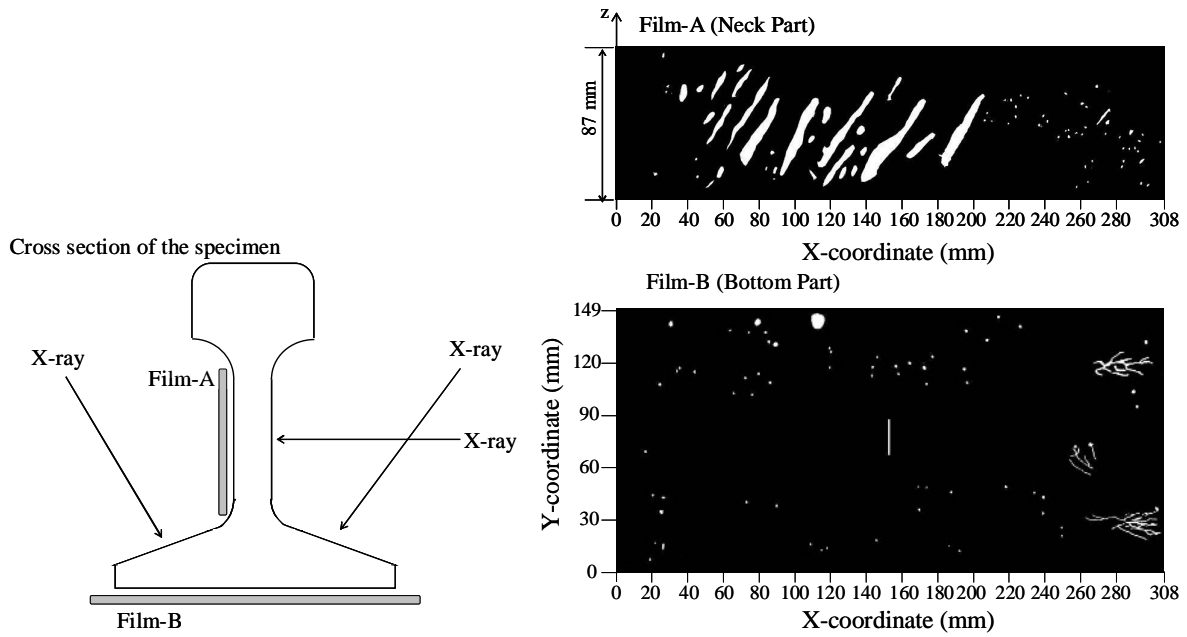


Fig.6 Results of radiographic testing for the specimen.

3.2 Experimental Setup and Equipment

The ultrasonic image of a certain plane is constructed by aperture synthesis method using ultrasonic signals detected at around the edge on the certain plane by pulse-echo method. The ultrasonic image of x-y plane was observed by scanning the ultrasonic transducer on y-z plane along y-axis at $z=6.5\text{mm}$ (shown in Fig.7 as Type-A). The flaw image of z-x plane was observed by scanning the transducer on y-z plane along z-axis at $y=72\text{mm}$ (Type-B). The flaw image of x-y plane was also observed by scanning the transducer on z-x plane along x-axis at $z=6.5\text{mm}$ (Type-C). The scan pitch of the sensor was 5mm. Ultrasonic wave was excited by spike pulse of -450V from the Pulser/Receiver (PANAMETRICS-NDT MODEL 5072PR) at each point. The specification of the transducer used in this experiment is shown in Table 1. Data acquisition is conducted by A/D converter (NI PXI-5122 14Bit digitizer) whose sampling rate is 100MHz.

Figure 8 shows the wavelet contour map for the ultrasonic signal shown in Fig.1. This figure reveals high-frequency components of around 8MHz are overlapped with main components of around 2.25MHz. Then, frequency components of 2.25MHz were extracted and used for constructing the ultrasonic image.

Table 1 Specification of transducer used in this experiment.

Model number	SFZ57A2276
Manufacturer	Automation Industries
Nominal Frequency	2.25MHz
Band width	Narrow Band
Diameter	0.5 inch

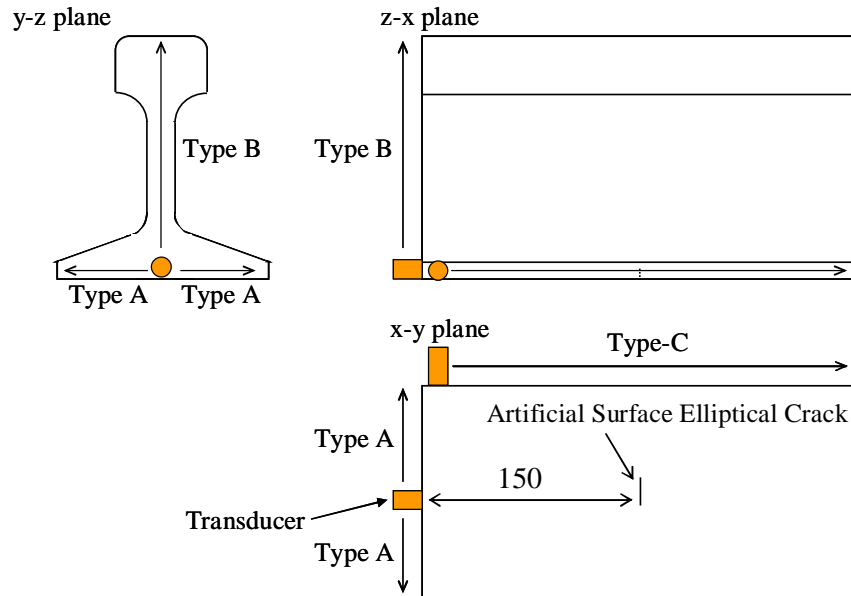


Fig.7 Three types of scan direction.

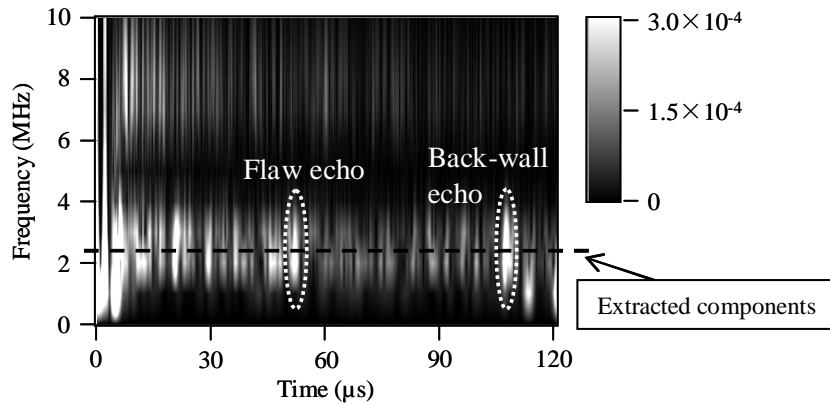


Fig.8 The contour map of wavelet transform (time-frequency analysis) for the ultrasonic signal shown in Fig.1.

4. Experimental result and discussion

Figure 9 shows the ultrasonic image of x-y plane by scanning sensor along y-axis at $z=6.3\text{mm}$ (Type A in Fig.7). The left figure was constructed by conventional aperture synthesis method and the right by proposed method. Due to the attenuation of ultrasonic beams, brightness of both figures becomes gradually dark along x-coordinate. Figure 10 shows the average amplitude of each point which is same distance from the inspection surface ($x=0\text{mm}$) along x-coordinate in Fig.9. Brightness of the image at each point was normalized as the amplitude-range became 0 to 1. After the normalization of ultrasonic images, both the brightness and the contrast of ultrasonic were adjusted by a commercial software (Adobe® Photoshop® Elements 4.0).

Figure 11 to 13 are ultrasonic images of x-y plane (scan pattern was type-A in Fig.7), z-x plane (Type-B) and x-y plane (Type-C) after the normalization and the image processing. The applied conditions for the image processing are shown in Table 2. High intensity points (white portion) are uniformly distributed in the ultrasonic images by the conventional aperture synthesis method (left of the figures). Any useful information cannot be obtained from these images. On the other hand, ultrasonic images by the proposed method roughly show distributions of defects. These distributions roughly match to those obtained by radiographic testing shown in Fig.6. For example, in Fig.11, a large number of white portions are observed at near the upper rim (location-B). In Fig.12, a void group is observed at location-B. In Fig.13, large dendritic defects are observed at location-B. These tendencies correspond to the results by radiographic testing (Fig.6). When mention is made of crack,

only the edges of the artificial flaw can be observed at the location “A” in the figures, while we had assumed that the line-shaped flaw appeared in the image. It seems difficult to find the cracks from the images without additional information. Even if the defect could be detected at location-A in Fig.11 and 13, we may misjudge planar cracks as point-shaped casting cavity from the image.

To summarize the results, we can conclude as follows.

1. Distribution of large defects in the high-manganese steel rail can be roughly observed by the proposed method.
2. The artificial semiellipse surface crack of 19.8mm-length and 6.5mm-depth seems difficult to find by the proposed method without additional information.
3. Even if the defect could be detected, planar cracks may be misjudged as point-shaped defects by the proposed method.

Even if the ultrasonic images obtained by aperture synthesis are improved by the proposed method, further investigations are required for applying UT to the real high manganese steel rails in field.

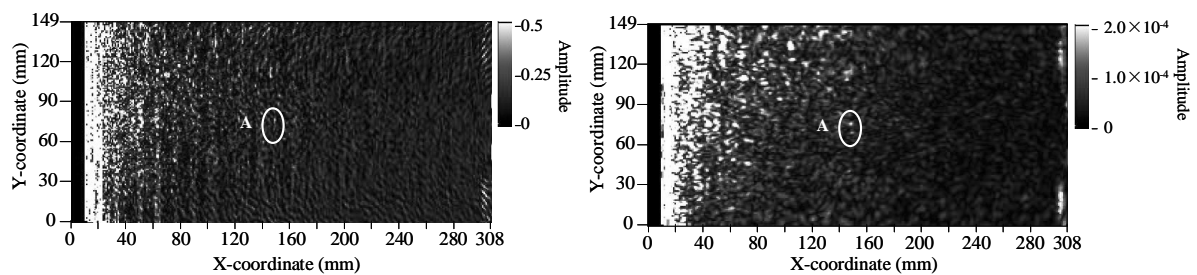


Fig.9 Flaw image of x-y plane at $z=6.3\text{mm}$ (scan pattern: type-A) without normalization.

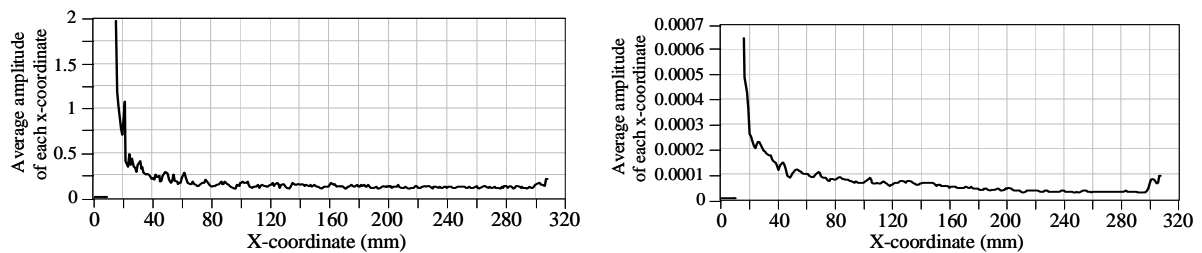


Fig.10 Average amplitude of each x-coordinate.

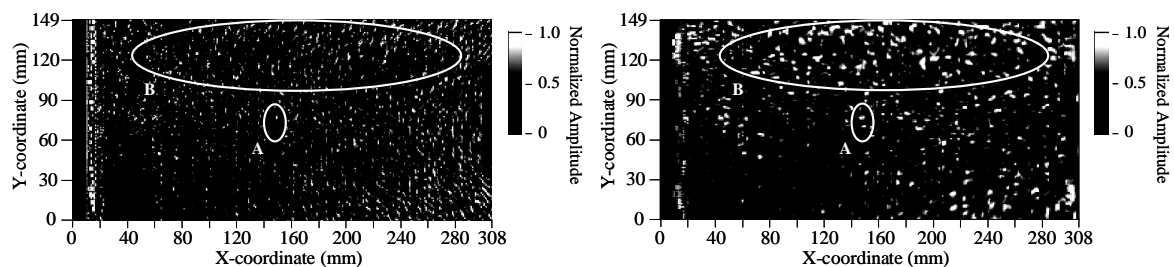


Fig.11 Flaw image of x-y plane at $z=6.3\text{mm}$ (scan pattern: type-A) with normalization.

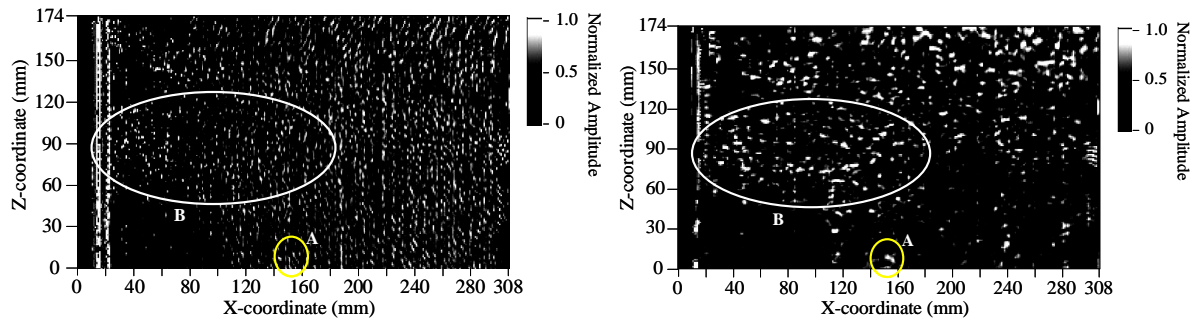


Fig.12 Flaw image of z-x plane at y=78mm (scan pattern: type-B) with normalization.

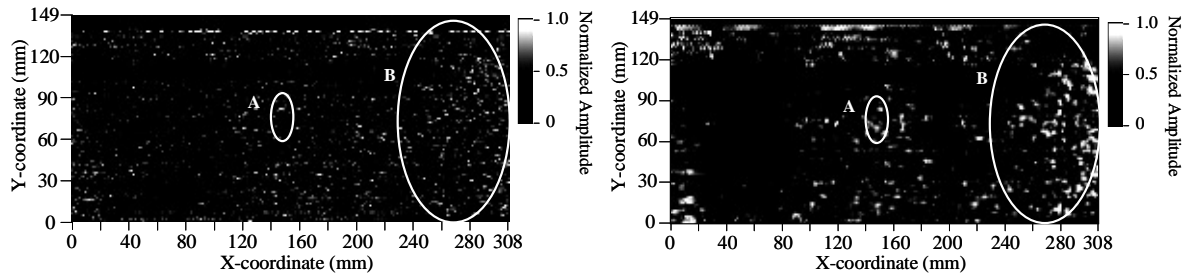


Fig.13 Flaw image of x-y plane at z=6.3mm (scan pattern: type-C) with normalization.

Table 2 The condition of image processing.

Fig. number	Adjustment for Brightness	Adjustment for Contrast
Fig.11	-40	+60
Fig.12	-35	+60
Fig.13	-30	+50

Unit: %

4. Conclusion

In this study, in order to make UT applicable to high manganese steel rails, a hybrid aperture synthesis method utilizing wavelet transform was proposed. The high manganese casting steel rail with an artificial semielliptical surface crack of 19.8mm length and 6.5mm depth was prepared for the study. The results are summarized as follows;

1. The aperture synthesis ultrasonic image was improved by applying the proposed method.
2. Distributions of large defects can be roughly observed by the proposed method, while small cracks will be undetected.
3. Planar cracks may be misjudged as point-shaped defects by the proposed method.
4. Further investigations are required for applying UT to the high-manganese steel rails in field.

Acknowledgement

The specimen used for this study was provided by Eikura communication Ltd.

Reference

- [1] Ryuta HIROKAWA et.al, Fundamental Investigation of an Ultrasonic Inspection Method Applicable to High Manganese Steel Rails, Proceedings of ASNT Fall Conference, 2007
- [2] Yasuo KUROSUMI, Development of Ultrasonic Inspection Technique for Casting Stainless Steel, INSS JOURNAL, Vol.7, 2000, p.159-171
- [3] M.Serre et.al, Ultrasonic Examination of Cast Stainless Steel, Proceedings of 12th ICNDE in the Nuclear and Pressure Vessel Industries, 1993, p.191-196
- [4] N.M.Bigutai et.al, The Effect of Grain Size on Flaw Visibility Enhancement using Split Spectrum Processing, Material Evaluation, Vol.42, No.5, May 1984, p.808-814
- [5] C.Poidevin et.al, Ultrasonic Examination of Cast Stainless Steel, Proceedings of 14th ICNDE in the Nuclear and Pressure Vessel Industries, 1996, p.575-581